HHS Public Access

Author manuscript

Biomaterials. Author manuscript; available in PMC 2018 January 01.

Published in final edited form as:

Biomaterials. 2017 January ; 112: 20–30. doi:10.1016/j.biomaterials.2016.10.007.

Modular GAG-matrices to promote mammary epithelial morphogenesis *in vitro*

Mirko Nowak[a], **Uwe Freudenberg**[a], **Mikhail V. Tsurkan**[a], **Carsten Werner**[a], and **Kandice R. Levental**[a,b,*]

[a] Leibniz Institute of Polymer Research Dresden e.V., Max Bergmann Center of Biomaterials Dresden, Center for Regenerative Therapies Dresden, TU Dresden, Germany

[b] Department of Integrative Biology and Pharmacology, McGovern Medical School at the University of Texas Health Science Center at Houston, Houston, TX USA

Abstract

Matrix systems used to study complex three-dimensional (3D) cellular processes like mammary epithelial tissue morphogenesis and tumorigenesis *ex vivo* often require ill-defined biological components, which lead to poor reproducibility and a lack of control over physical parameters. In this study, a well-defined, tunable synthetic biohybrid hydrogel composed of the glycosaminoglycan heparin, star-shaped poly(ethylene glycol) (starPEG), and matrix metalloproteinase- (MMP-) cleavable crosslinkers was applied to dissect the biophysical and biochemical signals promoting human mammary epithelial cell (MEC) morphogenesis. We show that compliant starPEG-heparin matrices promote the development of polarized MEC acini. Both the presence of heparin and MMP-cleavable crosslinks are essential in facilitating MEC morphogenesis without supplementation of exogenous adhesion ligands. In this system, MECs secrete and organize laminin in basement membrane-like assemblies to promote integrin signaling and drive acinar development. Therefore, starPEG-heparin hydrogels provide a versatile platform to study mammary epithelial tissue morphogenesis in a chemically defined and precisely tunable 3D *in vitro* microenvironment. The system allows investigation of biophysical and biochemical aspects of mammary gland biology and potentially a variety of other organoid culture studies.

Keywords

Mammary epithelium; Cell-material interaction; Organoid morphogenesis; Heparin; Biomimetic material

* corresponding author: kandice.r.levental@uth.tmc.edu, fax: 1-713-500-7456.

Introduction

Mammary gland development and homeostasis are tightly regulated and depend on diverse instructive signals from a highly complex biochemical and biophysical extracellular microenvironment. In the last two decades, three-dimensional (3D) *in vitro* culture models of mammary morphogenesis have successfully contributed to deciphering the mechanisms underlying crucial aspects of mammary epithelial development and tumorigenesis (reviewed in [1-4]). However, most 3D *in vitro* mammary epithelial studies have been conducted using biologically-derived extracellular matrix (ECM) biomaterials, such as a basement membrane extract (BME, commercially known as Matrigel®) or hydrogels which self-assemble from the fibrillar ECM protein collagen I. In addition to their self-assembly into soft, 3D scaffolds, both of these matrices either contain or include exogenously supplemented ligands such as laminin (LN) to recapitulate aspects of the native basement membrane of epithelial cells. Non-transformed mammary epithelial cells (MECs, e.g. MCF10A cell line) embedded as single cells in these biologically-derived matrices proliferate and develop into growth-arrested, polarized multi-cellular spherical organoids, which closely resemble the terminal ductal lobular units (acini) of the native human mammary epithelium (Fig. 1A) [2, 5-8]. Because of this remarkable recapitulation of native morphogenesis, BME has been the “gold standard” culture platform for modeling *ex vivo* mammary epithelial development.

Despite their utility, naturally-derived biomaterials have several significant intrinsic limitations, most notably a xenogeneic origin and a complex, ill-defined composition [9]. Furthermore, natural biomaterials lack methodological flexibility. For example, it is difficult to independently modulate their mechanical and biochemical properties, which limits their utility for measuring the impact of these cell-instructive microenvironment cues on cellular development and homeostasis. These limitations have profound impacts on cell response, experimental outcome, reproducibility, and comparative studies (reviewed in [3, 9]).

In response to these limitations, numerous synthetic biomaterials have been successfully engineered for 3D cell culture and tissue engineering applications [10-12]. Two commonly used synthetic biomaterials are poly(ethylene glycol)-(PEG) based hydrogels functionalized with specific cell-adhesion and degradation motifs and materials which self-assemble from peptides into fiber-like matrices. Only a few of these materials have been specifically designed or adapted to study 3D MEC morphogenesis [13-15], and these attempts have often lacked the design flexibility to independently examine various matrix properties. Thus, well-defined 3D synthetic matrices that allow the systematic investigation of the distinct contributions of biochemical and mechanical signals would be of great utility in investigations of the molecular events that drive MEC organogenesis and dysfunction.

To this end, we developed a modular and multifunctional glycosaminoglycan- (GAG-) based matrix system wherein the mechanical and biochemical properties of the matrix are precisely and independently tuned to study their effects on mammary epithelial morphogenesis [16, 17]. GAGs are major components of ECMs and are involved in diverse biological processes, including growth factor presentation, ECM assembly, and cell adhesion [18, 19]. Incorporation of the GAG heparin into synthetic matrices allows precise control of biochemical properties, e.g. biomimetic application of growth factors and presentation of

cell adhesion binding sites [17, 20-22]. The glycosaminoglycan building block is crosslinked by inert multi-arm starPEG or starPEG-peptide conjugates with a cell-degradable, matrix metalloproteinase-(MMP-) cleavable peptide sequence (GPQG↓IWGQ, the arrow indicating the cleavage site). This sequence is cleaved by numerous cell-secreted MMPs, including MMP-2 and MMP-3 [23], which are expressed by MECs [24] and play an important role in matrix remodeling during *in vivo* mammary epithelium growth and development [25].

Heparin and starPEG functionalized with MMP-cleavable sequences can be assembled *in situ* in the presence of cells via a mild and non-toxic Michael-type addition reaction to form a cell-compatible, multi-functional 3D polymeric hydrogel network (PEG-HEP; Fig. 1B) [16]. The relative concentration of these building blocks can be tuned to vary the extent of crosslinking, and thus matrix physical properties, independent of bulk heparin concentration. Further, these modular biohybrid materials have the design flexibility to substitute individual biofunctional components (e.g. peptide sequence, heparin), while keeping other key matrix parameters constant to independently investigate the role of each component in cellular morphogenesis [16]. In this work, we used PEG-HEP matrices to independently and systematically evaluate the influence of matrix degradability, physical properties (e.g. stiffness), and biochemical composition in *ex vivo* MEC morphogenesis (Fig. 1C).

Materials and methods

Cell culture

The non-malignant human mammary epithelial cell-line MCF10A (ATCC) was used between passages 4-20 and cells were maintained in DMEM/F-12 (Gibco) supplemented with 5% (v/v) horse serum (Invitrogen), 20 ng/ml epithelial growth factor (EGF, PeproTech), 0.5 μg/ml hydrocortisone (Sigma-Aldrich), 0.1 μg/ml cholera toxin (Sigma-Aldrich), 10 μg/ml insulin (Sigma-Aldrich), 1% (v/v) penicillin/streptomycin (Sigma-Aldrich) and were cultivated at 37°C and 5% CO_2 as described earlier[2].

Hydrogel formation

Four-armed star-shaped polyethylene glycol (PEG) maleimide (PEG-Mal, MW: 10080, JenKem) was functionalized with a matrix metalloproteinase (MMP)-sensitive peptide sequence (GCG **GPQG↓IWGQ** GGCG) (arrow indicates the site of proteolytic cleavage, bold letters indicate the cleavable peptide sequence, in house synthesis) at the terminal end of each PEG arm for cell mediated proteolytic matrix degradation (PEG-MCP; MW: 15920, JenKem with in-house peptide conjugation). Heparin (MW: ~15000, Calbiochem, in house maleimide functionalization) was functionalized with 6 maleimide groups per heparin molecule (HEP-Mal). The synthesis and characterization of these components was carried out as previously described [16, 26]. The mechanical properties of the matrices were modulated by cross-linking degree adjustment of PEG to heparin molar ratio (cPEG/cHEP, [γ]). Briefly, heparin functionalized with maleimide groups was dissolved in phosphate buffered saline (PBS; pH 5.5) and then mixed with cells. PEG-MCP was dissolved in the appropriate amount of PBS (pH 5.5). The heparin-cell solution was quickly mixed with the PEG-MCP solution, and 50 μl of the cell-gel reaction solution was directly cast in standard cell culture 96-well plates. The matrices polymerized within one min to form a covalently

cross-linked hydrogel. The pH of the PBS in which the precursors were dissolved in was decreased to pH 5.5 to increase the hydrogel gelation time for improved handling. After 15 min of polymerization in the incubator at 37°C, 200 μl growth medium was added on top of the gels and was changed every 2-3 days. Unless otherwise stated, all materials contain the MMP-cleavable peptide and are cell-degradable. To form non-degradable control matrices (PEG-scr-HEP), the MMP-degradable peptide sequence was replaced by a MMP-insensitive scrambled *(*scr*)* peptide sequence (GCG **IGQGQGPW** GGCG) (bold letters indicate the scrambled peptide sequence; in house synthesis) and were prepared similar to the gels containing PEG-MCP. To form non-heparin-containing PEG-PEG gels, the heparin-maleimide was replaced by four-armed starPEG-maleimide (PEG-Mal, MW: 10080, JenKem) which contains a reactive maleimide terminal group on each PEG arm. This polymer network was assembled by a Michael-type addition reaction of the free thiol-containing cysteine from the PEG-MCP reacting with the maleimide functional group from the PEG-Mal (same reaction mechanism as the PEG-heparin gels). The mechanical properties of the PEG-PEG gels were modulated via solid content adjustment with 2.5% (w/v) of polymer dry mass at a stoichiometric PEG-MCP (or PEG-scr) to PEG-Mal ratio of 1:1 to achieve similar mechanical properties (storage modulus of ~200 Pa) to soft PEG-HEP gels. The final cell concentration of encapsulated MECs in the hydrogels was 6.5×10^6 cells/ml. For MEC morphogenesis experiments in basement membrane extract (BME, Matrigel, BD Biosciences) gels cells were embedded in 50 μl BME as it has been described previously [2].

Table I summarizes all matrices used in this study. For simplicity, the following acronyms will be used in this manuscript: PEG-HEP defines MMP-cleavable heparin-based hydrogels consisting of PEG-MCP crosslinked to HEP-Mal. PEG-scr-HEP represents MMP-insensitive heparin-based hydrogels consisting of the precursors PEG-scr and HEP-Mal. PEG-PEG defines MMP-cleavable PEG-based hydrogels consisting of PEG-MCP and PEG-Mal. PEG-scr-PEG represents MMP-insensitive PEG-based hydrogels made from the crosslinking of PEG-scr to PEG-Mal.

Mechanical properties of hydrogels

The mechanical properties (storage modulus, reported in Pa) of the synthetic matrices and BME were determined by oscillatory shear measurements, carried out on an Ares LN2 rheometer (TA Instruments) equipped with an 8 mm parallel plate geometry. Measurements were carried out on gel discs which were swollen to equilibrium over 24 hours (resulting in approx. 1.3 mm thick samples). These swollen hydrogels were punched out using an 8 mm biopsy puncher. For BME rheological analysis, 60 μl BME was cast in cylindrical glass molds (8 mm diameter), polymerized for 30 min at 37°C and transferred to the lower rheometer plate for measurements. Dynamic frequency sweeps were carried out at 25°C over a range of 0.01-100 rad-s^{-1}, with an applied strain of 2-3%; the storage modulus of each material was taken as the mean value over this frequency range. A strain sweep experiment was performed to confirm that the applied strain value was within the linear viscoelastic regime of the tested materials. At least three gels per condition were measured, and the mean values of the storage modulus were calculated and reported.

Immunofluorescence analysis

Samples were briefly washed with PBS and fixed with 2% (w/v) paraformaldehyde (PFA, Sigma Aldrich) for 30 min at room temperature (RT) and then washed three times for 3 min each with PBS containing 0.1 M glycine (Sigma-Aldrich). Gels with cells were either embedded in optimal cutting temperature compound (Tissue-Tek-O.C.T, Sakura), frozen, and cut into 10-20 μm cryosections with a cryostat (HM 560, Leica Biosystems) or were directly stained in the hydrogels.

For immunofluorescence analysis, samples were permeabilized with 0.1% (v/v) Triton X-100 (Sigma-Aldrich) and blocked for 1 hr at RT with 5% (v/v) serum matching the secondary antibody host. Primary antibodies were then applied in blocking buffer for 2 hr at RT or overnight at 4°C, and subsequently the gels were washed three times for 15 min with PBS. Antibodies directed against the following antigens were used in this study: β-catenin (BD Pharmingen 610153; 1:100), β_4-integrin (Santa Cruz sc-9090; 1:100), GM130 (Golgi apparatus; BD Pharmingen 558712; 1:10), laminin-332 (α-3 chain, clone BM165, kindly provided by Peter Marinkovich of Stanford University), laminin-111 (α-1 chain; Santa Cruz sc-6016, 1:200). Secondary antibodies, Alexa fluor 488 or Alexa fluor 546 (Molecular Probes, 1:200; shown in green or red in the Figures, respectively), matching the primary antibody host species were diluted in blocking buffer and mixed with Alexa fluor 633 phalloidin (Molecular Probes, 1:50; shown in red in the Figures) to stain F-actin filaments. In these studies, β_4-integrin and the GM130 are labeled with Alexa Fluor 546 and shown in red in the figures; β-catenin, LN-332, and LN-111 are labeled with Alexa Fluor 488 and shown in green in the figures. The secondary antibodies were applied for 1 hr and subsequently washed three times for 15 min with PBS. Finally, the nuclei was counter-stained with 4′,6-diamidino-2-phenylindole (DAPI, Sigma-Aldrich, 1:10,000; shown in blue in the Figures) for 10 min and subsequently washed three times for 5 min at RT with PBS. As a negative control and to validate specificity, the secondary antibodies were tested on hydrogel samples without primary antibody incubation. Images were taken with a confocal laser scanning microscope (SP5; Leica Microsystems, Germany).

Immunohistological analysis

Mid-plane cross-section images were analyzed using ImageJ (1.49, NIH) and classified as *"not cleared"* if >3 cells were inside the luminal space. For the quantification of Golgi apparatus orientation, acini in which the Golgi apparatus was oriented in the outer cell layer in the direction of the lumen (as oriented by DAPI co-staining) were classified as "apically oriented", whereas colonies which displayed >3 Golgi apparatus directed towards the basolateral side were classified as "mislocalized" (non-polar organization). ~30 acini were examined for each condition in three independent experiments.

Morphometric analysis

Bright field images were acquired using a light microscope (Olympus IX50, 10x objective), and the diameter or area was determined by manually tracing the outline of ~150 acini and analyzed using ImageJ. Acini were classified as *"invasive"*, if they displayed an invading or ductal morphology on the bright field images.

Functional integrin blocking

For functional integrin blocking studies antibodies directed against human integrin subunit β_1 (BD Biosciences 552828) and integrin heterodimer $\alpha_6\beta_4$ (α_6 (BD Biosciences 555734), β_4 (Millipore MAB2059)) were added to the PEG-MCP precursor solution and to the cell culture media at a final concentration of 20 μg/ml.

Transmission electron microscopy

Hydrogel-cell constructs were fixed in modified Karnovsky's fixative (2% glutaraldehyde + 2% paraformaldehyde in 50 mM HEPES) for 30 min, dissected into small pieces in fixative under the fume hood and left in fixative overnight at 4°C. Samples were washed two times in 100 mM HEPES and two times in water, postfixed in 1% OsO_4/water for 2 hr on ice, washed several times with water, and *en bloc* contrasted with 1% uranyl acetate/water for 2 hr on ice. The samples were then washed several times in water, dehydrated in a graded series of ethanol/water up to 100% ethanol, infiltrated in epon 812 (epon/ethanol mixtures: 1:3, 1:1, 3:1 for 1.5 h each, pure epon overnight, pure epon 3 h), embedded in flat embedding molds, and cured at 65°C. Ultrathin sections were prepared with a Leica UC6 ultramicrotome (Leica Microsystems, Vienna, Austria), collected on formvar-coated slot grids, stained with lead citrate and uranyl acetate according to Venable and Coggeshall [27], and analyzed on a FEI Morgagni D268 (FEI, Eindhoven, The Netherlands) at 80 kV acceleration voltage.

Statistical analysis

All data were statistically analyzed using Prism software (version 6.04, GraphPad). If multiple data sets were compared, statistical significance was tested, depending on the normal distribution of data assessed by D'Agostino test, either by performing a one-way analysis of variance (ANOVA) with Tukey test for multiple comparisons or Kruskal-Wallis test with Dunn's multiple comparisons. If two data sets were compared a students' unpaired t-test was applied for statistical comparison. Levels of significance were determined as n.s. = not significant ($p \geq 0.05$); * $p < 0.05$; ** $p < 0.01$; *** $p < 0.001$.

Results

MEC morphogenesis in soft PEG-HEP matrices

We have utilized PEG-HEP matrices to determine the biochemical and biophysical cues necessary for the survival and morphogenesis of several cell types, including endothelial cells [16, 20, 22, 26], neurons [16], and pancreatic islets [28]. Therefore, we hypothesized that PEG-HEP hydrogels could be an exemplary matrix to study the interplay between the microenvironment and complex mammary epithelium multi-cellular morphogenesis in a 3D *in vivo*-like context. To this end, MECs (the MCF10A cell line) were embedded as single cells within degradable PEG-HEP matrices, without supplementation of exogenous adhesive or signaling ligands (e.g. basement membrane proteins or adhesive peptides). To mimic the mechanical properties of the normal stroma adjacent to the mammary epithelium [29] and the reference BME, the PEG-HEP matrix mechanical properties were adjusted by tuning the crosslinking degree of the hydrogel. A molar ratio of PEG to heparin (γ) of 0.63 yielded

matrices with a stiffness indistinguishable from BME (storage modulus of ~200-350 Pa), while increased PEG levels yielded stiffer materials (storage modulus of ~1600 Pa, Fig. 2A), as expected [16].

MECs cultured in soft, enzymatically degradable PEG-HEP hydrogels developed within 6-8 days into growth-arrested, spherical colonies (Fig. 2B top row) with growth characteristics similar to the reference BME (Supplementary Fig. S1A and S1B). Immunofluorescence analysis of cross sections of MEC acini after 14 days of culture revealed that the colonies were polarized, as indicated by typical epithelial apicobasal polarization marker distribution – lateral β-catenin, basal β_4 integrin, and extracellular LN-332 deposition on the basal surface (Fig. 2B, middle and bottom row). Furthermore, a high percentage of colonies showed luminal clearance (58 ± 3%; Fig. 2C) and had their Golgi apparatus oriented towards the apical side of the constructs (85 ± 3%; Fig. 2D), both indicative of normal MEC morphogenesis. The polarized epithelial tissue architecture was comparable to MECs cultured in BME. Ultrastructural transmission electron microscopy (TEM) analysis of MECs cultured within the soft PEG-HEP hydrogels revealed the presence of abundant, epithelial cell-characteristic desmosomes [30] as dense structures parallel to the lateral plasma membrane at the cell-cell interface which are connected to a dense network of cytoplasmic intermediate filaments (Fig. 2F). TEM analysis also showed the formation of hemidesmosomes, which are dense plaques that connect several laminin isoforms of the basement membrane to the basal surface of the cells via $\alpha_6\beta_4$ integrins (Fig. 2G) [31, 32]. These polarized architectural features are consistent with those previously reported for MECs cultured in BME [33].

Polarized acini developed within soft PEG-HEP matrices even without supplementation of exogenous adhesion ligands or differentiation cues. These results are striking given that previous 3D synthetic cultures of MECs have required expensive, ill-defined exogenous biochemical stimuli to promote MEC morphogenesis and acini polarization. By overcoming this constraint, we demonstrate that soft, MMP-degradable PEG-HEP hydrogels are a compositionally and structurally defined alternative for BME, which support not only MEC viability and growth but also the formation of multi-cellular polarized mammary epithelial organoids.

Impact of matrix stiffness on MEC morphogenesis in PEG-HEP matrices

Matrix stiffness critically influences MEC development, with increased substrate stiffness perturbing morphogenesis and epithelial integrity (loss of polarized organization), and promoting an invasive tumor-like phenotype [13, 29]. One key design feature of the PEG-HEP hydrogels is facile tuning of matrix physical properties independent of the biochemical environment (e.g. adhesion ligands, growth factors, etc.) [16, 17]. To assess the impact of biophysical properties of PEG-HEP matrices on MEC morphogenesis, the stiffness (storage modulus) of the hydrogels was increased to 1600 ± 350 Pa (Fig. 2A), similar to the stroma of early breast tumors [29], by increasing the crosslinking degree (γ = 1.25).

In contrast to soft PEG-HEP matrices, MECs in stiff PEG-HEP hydrogels proliferated more, as indicated by the increased colony cross-sectional area after two weeks of culture (Supplementary Fig. S2A). Growing cells in stiff matrices also resulted in a high percentage

of colonies lacking a cleared luminal space, indicative of enhanced luminal cell survival (Fig. 2C). These colonies also showed a loss of epithelial organization, as indicated by diffuse and unorganized β-catenin and β_4 integrin staining (Fig. 2B, right middle and bottom rows), in agreement with previous reports [13, 14, 29, 34]. Notably, ~30% of the colonies in stiffer PEG-HEP matrices developed into an “invasive” phenotype (Fig. 2B, right and 2E), which was not observed in soft PEG-HEP matrices.

Impact of matrix degradability and GAG inclusion on MEC morphogenesis

MMPs are critical mediators of matrix degradation and remodeling during MEC development [35, 36]. To validate the functional relevance of cell-mediated matrix remodeling in the formation of acini in PEG-HEP matrices, the MMP-cleavable peptide sequence was replaced with a scrambled MMP-insensitive peptide sequence (IGQGQGPW). The mechanical properties were matched to the soft PEG-HEP matrices by adjusting the crosslinking degree (γ=0.63) (Fig. 3A) to exclude effects of matrix stiffness on acini development.

MECs embedded in soft, non-cleavable PEG-scr-HEP matrices grew into spherical colonies (Fig. 3B) with similar growth kinetics and final colony size as the parallel enzymatically cleavable matrices (PEG-HEP) (Fig. 3D and Supplementary Fig. S1B). Additionally, in both cleavable and non-cleavable soft PEG-HEP matrices, LN-332 was secreted and deposited on the basal colony surface (Fig. 3C, bottom center). However, morphogenesis of the cells grown in the nondegradable materials was perturbed, as indicated by disrupted β_4 integrin and β-catenin localization (Fig. 3C, top center), aberrant luminal clearance (Fig. 3E), and mislocalized Golgi apparati (Fig. 3F).

To investigate the necessity of the GAG building-block in MEC morphogenesis, we analyzed hydrogels in which heparin was substituted with biologically inert PEG. To isolate the effect of heparin, we maintained the enzymatic degradability and matrix mechanical properties by incorporating the MMP-cleavable peptide sequence (GPQG↓IWGQ) and adjusting the physical properties to match the soft PEG-HEP matrices (Fig. 3A). MECs embedded in soft, degradable PEG-PEG matrices survived, but either failed to proliferate (i.e. remained as single cells) or grew into small non-polarized clusters (Fig. 3B and D, right) with highly disorganized β-catenin and β_4 integrin distribution, sparse and non-continuous deposition of LN-332 (Fig. 3C, right), and a lack of luminal clearance (Fig. 3E). Finally, MECs cultured in non-cleavable PEG-scr-PEG gels did not grow (Supplementary Fig. S2B), further emphasizing the necessity of the cleavable MMP-sensitive sequence. These data clearly indicate that both the MMP-degradable peptide sequence and the GAG heparin are crucial building blocks for MEC morphogenesis in soft PEG-HEP hydrogels.

MEC morphogenesis in soft PEG-HEP hydrogels guided by cell-material interactions

LN-111 and LN-332, components of the mammary epithelium basement membrane *in vivo*, have been shown to be important regulators of proper mammary epithelium development and functional differentiation [6, 37, 38]. Accordingly, previous studies of MEC morphogenesis in 3D *in vitro* culture platforms have relied on exogenous LN-111, either as an intrinsic component of BME or supplied as a purified protein [13, 14, 39]. In these *in*

vitro models, exogenous LN-111 promotes initial cell adhesion and is necessary for the signaling that drives mammary epithelial development [6, 7].

In soft, degradable PEG-HEP matrices, MECs developed into polarized acini-like structures without exogenous LN supplementation. Therefore, we investigated the cell-material interactions responsible for MEC morphogenesis in these materials. Confocal imaging and immunofluorescence analysis after two days of culture in soft, MMP-cleavable PEG-HEP hydrogels revealed that LN-332 was secreted by the cells, but was not fully distributed around the basal surface of the colony at this stage of development. However, by day 4, the distribution of LN-332 around the outer colony surface was continuous (Fig. 4A, top). Surprisingly, LN-111 could not be detected basally during the course of development (Fig. 4A, bottom row, see positive control staining Supplementary Fig. S3).

Integrins are transmembrane cell surface receptors for extracellular matrix proteins and are responsible for transducing cellular adhesion into intracellular signals that regulate many cellular processes [40], including those involved in MEC morphogenesis and mammary gland development [41, 42]. To determine if integrin binding to the LN-332 that is secreted and assembled by the MECs in the PEG-HEP matrices is necessary for mammary morphogenesis, we used functional blocking antibodies against the β_1 integrin subunit, which is involved in mammary epithelium integrin-matrix interactions via $\alpha_6\beta_1$ and $\alpha_3\beta_1$, and against the hemidesmosomal $\alpha_6\beta_4$ integrin heterodimer, which interacts with both LN-111 and -332 [43, 44]. Colony growth was significantly inhibited by both $\alpha_6\beta_4$ and β_1 integrin blocking antibodies, suggesting that MEC morphogenesis was disrupted (Fig. 4B-D). These results demonstrate that MECs secrete LN-332 during morphogenesis in soft PEG-HEP hydrogels, and that binding of β_1 and $\alpha_6\beta_4$ integrins to this cell-secreted LN is necessary for polarized acini development (Fig. 4E).

Discussion

Determining the factors that drive organogenesis *ex vivo* is of supreme interest for understanding the mechanisms behind tissue development and pathologies *in vivo* and for development of tools for drug discovery and regenerative therapies. Recently, embryonic and adult stem cell-driven differentiation and tissue assembly *in vitro* have offered mechanistic insights into the factors necessary for organogenesis [45-47]; however, these systems have failed to completely recapitulate organ development *in vivo*. This failure may be due in part to poorly controlled extracellular matrix preparations in organoid cultures. This limitation could be overcome by the use of defined, tunable, and reproducible synthetic or biohybrid matrix systems, which may more successfully mimic native organotypic scaffolds *in vivo*.

Here, we applied a well-defined, widely tunable, modular synthetic hydrogel platform [16, 26, 48] to independently investigate the influence of physical cues (e.g. stiffness) and biochemical signals (e.g. presence of GAGs or enzymatically cleavable peptides) on mammary epithelial morphogenesis *in vitro*. MECs cultured in soft, MMP-cleavable PEG-HEP matrices had comparable growth characteristics, luminal clearing, and polarization to those observed in BME, the archetypal matrix for *ex vivo* recapitulation of mammary development. The mechanical properties of the stroma surrounding the mammary epithelium

are crucial regulators of mammary epithelium development, as well as malignant transformation and progression [13, 29, 34]. Consequently, we examined the effect of increased stiffness of PEG-HEP matrices and observed that the polarized architecture of mammary acini was perturbed in stiffened matrices, consistent with previous results [13, 29, 34].

Previous studies have shown that inclusion of laminin or BME into natural or synthetic matrices is necessary for proper MEC morphogenesis *in vitro* [6, 13, 14]. Surprisingly, in our matrices, polarized constructs formed in soft PEG-HEP hydrogels without any additional functionalization of the matrix with adhesive building-blocks (e.g. RGD, SIKVAV) or entrapment of exogenous basement membrane proteins (e.g. LN-111 or BME). To evaluate the mechanism underlying this unexpected finding, we investigated the cell-material interactions that are responsible for mammary development in soft PEG-HEP matrices. We found that by day 2 of culture, MECs secrete and organize LN-332 around the growing colonies, and that LN-332 is fully incorporated and homogeneously distributed around the developing acini by day 4. These results are consistent with previous studies where LN-332 was also incorporated into the basement membrane of developing MEC colonies after several days [6, 8]. Furthermore, we analyzed which integrins are involved in mediating morphogenesis in PEG-HEP hydrogels and found that the integrin-matrix interaction involving $\alpha_6\beta_4$ or β_1 integrins, both of which can bind LN [7, 49], are essential for MEC acinar morphogenesis.

We speculate that polarization of MECs in soft PEG-HEP matrices in the absence of exogenous LN or BME can be explained by two non-exclusive mechanisms: (1) LN-332 is constitutively secreted by cells and adsorbs to heparin, permitting ligation and activation of $\alpha_6\beta_4$ and β_1-containing integrins [43, 44]; or (2) heparin directly interacts with integrin receptor(s) (e.g. $\alpha_6\beta_4$ or β_1) to modulate initial cell adhesion, survival, and differentiation, as has been reported for the activation of integrins $\alpha_{IIb}\beta_3$ and $\alpha_5\beta_1$ by soluble and surface-immobilized heparin [50-53]. As LN-332 does not bind to collagen I [54, 55], previous attempts to recapitulate MEC morphogenesis with LN-332 may have failed due to its lack of incorporation / immobilization into the collagen matrices. Inclusion of heparin in PEG-HEP hydrogels provides a binding site for the secreted LN-332, and thus allows its assembly into the cell-secreted ECM.

Future studies will apply PEG-HEP matrices to establish a user-defined, heterotypic, 3D co-culture tissue model system towards recapitulation of the complex environment of the breast tissue by incorporating stromal cells (e.g. myoepithelial cells, adipocytes, immune cells, endothelial cells, and/or fibroblasts), which can interact by direct physical contact and/or paracrine signaling with the mammary epithelium [56, 57]. Furthermore, this strategy is potentially applicable to many other epithelial tissue engineering applications, including *ex vivo* culture of kidney or gut organoids. Determining how the microenvironment influences organ development, dysplasia, and malignant transformation in systematic and rational manner will allow researchers to identify crucial cues for normal morphogenetic processes and characteristic alterations in cancer.

Conclusion

In this study we have successfully applied a synthetic, tunable, modular GAG-based biohybrid material to investigate the influence of various matrix properties on mammary epithelial morphogenesis in a 3D, biomimetic context. This modular design is widely adaptable, for example by substitution of heparin with other GAGs, through tethering the matrix with specific ECM adhesion ligand peptides (e.g. RGD, SIKVAV), or via the inclusion of specific heparin-binding growth factors (e.g. TGFβ [58] or HGF [59]). This versatile culture platform has the necessary characteristics for defined and systematic investigations of mechanical properties and their crosstalk with biochemical cues to determine the individual signals that induce or suppress invasion and malignancy in the normal mammary epithelium.

Supplementary Material

Refer to Web version on PubMed Central for supplementary material.

Acknowledgements

The authors would like to thank Dr. Thomas Kurth from the Electron Microscopy Facility at Center for Regenerative Therapies Dresden (CRTD) for the excellent TEM processing and imaging and Marcus Binner (Leibniz Institute of Polymer Research Dresden) for material synthesis. This work was supported by the Deutsche Forschungsgemeinschaft through CRC TR 67 (UF, CW), CRC SFB 655 (CW), FR 3367/2-1 (UF), WE 2539-7 (CW), and FOR/EXC999 (CW), by the Leibniz Association through SAW-2011-IPF-2 68 (CW), by the European Union through the FP7 projects ANGIOSCAFF (grant agreement no. 214402-2, CW) and HydroZONES (grant agreement no. 309962, CW) and through the Federal Ministry of Education and Research of Germany through the initiative “Unternehmen Region Zwanzig20” project RESPONSE (FKZ 03ZZ0903E, CW) and initiative “Innovative Gesundheitstechnologien” project EXASENS (FKZ 13N13859, CW). KRL is supported by the National Institutes of Health (grant 1R01GM114282).

References

1. Debnath J, Brugge JS. Modelling glandular epithelial cancers in three-dimensional cultures. Nature reviews Cancer. 2005; 5:675–88. [PubMed: 16148884]
2. Debnath J, Muthuswamy SK, Brugge JS. Morphogenesis and oncogenesis of MCF-10A mammary epithelial acini grown in three-dimensional basement membrane cultures. Methods. 2003; 30:256–68. [PubMed: 12798140]
3. Johnson KR, Leight JL, Weaver VM. Demystifying the effects of a three-dimensional microenvironment in tissue morphogenesis. Methods in cell biology. 2007; 83:547–83. [PubMed: 17613324]
4. Lee GY, Kenny PA, Lee EH, Bissell MJ. Three-dimensional culture models of normal and malignant breast epithelial cells. Nature methods. 2007; 4:359–65. [PubMed: 17396127]
5. Barcellos-Hoff MH, Aggeler J, Ram TG, Bissell MJ. Functional differentiation and alveolar morphogenesis of primary mammary cultures on reconstituted basement membrane. Development (Cambridge, England). 1989; 105:223–35.
6. Gudjonsson T, Rønnov-Jessen L, Villadsen R, Rank F, Bissell MJ, Petersen OW. Normal and tumor-derived myoepithelial cells differ in their ability to interact with luminal breast epithelial cells for polarity and basement membrane deposition. Journal of cell science. 2002; 115:39–50. [PubMed: 11801722]
7. Muschler J, Lochter A, Roskelley CD, Bissell MJ. Division of labor among the alpha6beta4 integrin, beta1 integrins, and an E3 laminin receptor to signal morphogenesis and beta-casein expression in mammary epithelial cells. Molecular biology of the cell. 1999; 10:2817–28. [PubMed: 10473629]

8. Petersen OW, Rønnov-Jessen L, Howlett aR, Bissell MJ. Interaction with basement membrane serves to rapidly distinguish growth and differentiation pattern of normal and malignant human breast epithelial cells. Proceedings of the National Academy of Sciences of the United States of America. 1992; 89:9064–8. [PubMed: 1384042]
9. Hughes CS, Postovit LM, Lajoie Ga. Matrigel: A complex protein mixture required for optimal growth of cell culture. PROTEOMICS. 2010; 10:1886–90. [PubMed: 20162561]
10. Lutolf MP, Blau HM. Artificial stem cell niches. Advanced materials (Deerfield Beach, Fla). 2009; 21:3255–68.
11. Shastri VP, Lendlein A. Materials in Regenerative Medicine. Advanced Materials. 2009; 21:3231–4. [PubMed: 20882492]
12. Slaughter BV, Khurshid SS, Fisher OZ, Khademhosseini A, Peppas Na. Hydrogels in Regenerative Medicine. Advanced Materials. 2009; 21:3307–29. [PubMed: 20882499]
13. Chaudhuri O, Koshy ST, Branco da Cunha C, Shin J-w, Verbeke CS, Allison KH, et al. Extracellular matrix stiffness and composition jointly regulate the induction of malignant phenotypes in mammary epithelium. Nature Materials. 2014; 13:970–8. [PubMed: 24930031]
14. Miroshnikova YA, Jorgens DM, Spirio L, Auer M, Sarang-Sieminski AL, Weaver VM. Engineering strategies to recapitulate epithelial morphogenesis within synthetic three-dimensional extracellular matrix with tunable mechanical properties. Physical biology. 2011; 8:026013. [PubMed: 21441648]
15. Weiss MS, Bernabe BP, Shikanov A, Bluver DA, Mui MD, Shin S, et al. The impact of adhesion peptides within hydrogels on the phenotype and signaling of normal and cancerous mammary epithelial cells. Biomaterials. 2012; 33:3548–59. [PubMed: 22341213]
16. Tsurkan MV, Chwalek K, Prokoph S, Zieris A, Levental KR, Freudenberg U, et al. Defined Polymer-Peptide Conjugates to Form Cell-Instructive starPEG-Heparin Matrices In Situ. Advanced materials (Deerfield Beach, Fla). 2013; 25:2606–10.
17. Uwe Freudenberg, Jens-Uwe Sommer; Levental, Kandice R.; Welzel, Petra B.; Zieris, Andrea; Chwalek, Karolina, et al. Using Mean Field Theory to Guide Biofunctional Materials Design. Advanced Functional Materials. 2012; 22:1391–8.
18. Capila I, Linhardt RJ. Heparin-protein interactions. Angewandte Chemie. 2002; 41:391–412. [PubMed: 12491369]
19. Garg HG, Cowman MK, Hales CA. Biological Function of Glycosaminoglycans. Carbohydrate Chemistry, Biology and Medical Applications. 2011:209.
20. Zieris A, Chwalek K, Prokoph S, Levental KR, Welzel PB, Freudenberg U, et al. Dual independent delivery of pro-angiogenic growth factors from starPEG-heparin hydrogels. Journal of controlled release : official journal of the Controlled Release Society. 2011; 156:28–36. [PubMed: 21763368]
21. Zieris A, Dockhorn R, Rohrich A, Zimmermann R, Muller M, Welzel PB, et al. Biohybrid networks of selectively desulfated glycosaminoglycans for tunable growth factor delivery. Biomacromolecules. 2014; 15:4439–46. [PubMed: 25329425]
22. Zieris A, Prokoph S, Levental KR, Welzel PB, Grimmer M, Freudenberg U, et al. FGF-2 and VEGF functionalization of starPEG-heparin hydrogels to modulate biomolecular and physical cues of angiogenesis. Biomaterials. 2010; 31:7985–94. [PubMed: 20674970]
23. Nagase H, Fields GB. Human matrix metalloproteinase specificity studies using collagen sequence-based synthetic peptides. Biopolymers. 1996; 40:399–416. [PubMed: 8765610]
24. Giambernardi Ta, Grant GM.; Taylor GP, Hay RJ.; Maher VM, McCormick JJ., et al. Overview of matrix metalloproteinase expression in cultured human cells. Matrix biology : journal of the International Society for Matrix Biology. 1998; 16:483–96. [PubMed: 9550265]
25. Wiseman BS, Sternlicht MD, Lund LR, Alexander CM, Mott J, Bissell MJ, et al. Site-specific inductive and inhibitory activities of MMP-2 and MMP-3 orchestrate mammary gland branching morphogenesis. The Journal of cell biology. 2003; 162:1123–33. [PubMed: 12975354]
26. Chwalek K, Tsurkan MV, Freudenberg U, Werner C. Glycosaminoglycan-based hydrogels to modulate heterocellular communication in in vitro angiogenesis models. Scientific reports. 2014; 4:4414. [PubMed: 24643064]
27. Venable JH, Coggeshall R. A simplified lead citrate stain for use in electron microscopy. The Journal of Cell Biology. 1965; 25:407–8. [PubMed: 14287192]

28. Borg DJ, Welzel PB, Grimmer M, Friedrichs J, Weigelt M, Wilhelm C, et al. Macroporous biohybrid cryogels for co-housing pancreatic islets with mesenchymal stromal cells. Acta biomaterialia. 2016
29. Paszek MJ, Zahir N, Johnson KR, Lakins JN, Rozenberg GI, Gefen A, et al. Tensional homeostasis and the malignant phenotype. Cancer Cell. 2005; 8:241–54. [PubMed: 16169468]
30. Green KJ, Jones JC. Desmosomes and hemidesmosomes: structure and function of molecular components. The FASEB journal : official publication of the Federation of American Societies for Experimental Biology. 1996; 10:871–81. [PubMed: 8666164]
31. Sonnenberg A, Calafat J, Janssen H, Daams H, van der Raaij-Helmer LM, Falcioni R, et al. Integrin alpha 6/beta 4 complex is located in hemidesmosomes, suggesting a major role in epidermal cell-basement membrane adhesion. J Cell Biol. 1991; 113:907–17. [PubMed: 2026654]
32. Spinardi L. A recombinant tail-less integrin beta 4 subunit disrupts hemidesmosomes, but does not suppress alpha 6 beta 4-mediated cell adhesion to laminins. The Journal of Cell Biology. 1995; 129:473–87. [PubMed: 7721947]
33. Underwood JM, Imbalzano KM, Weaver VM, Fischer AH, Imbalzano AN, Nickerson JA. The ultrastructure of MCF-10A acini. Journal of cellular physiology. 2006; 208:141–8. [PubMed: 16607610]
34. Levental KR, Yu H, Kass L, Lakins JN, Egeblad M, Erler JT, et al. Matrix crosslinking forces tumor progression by enhancing integrin signaling. Cell. 2009; 139:891–906. [PubMed: 19931152]
35. Howard, Ba; Lu, P. Stromal regulation of embryonic and postnatal mammary epithelial development and differentiation. Seminars in cell & developmental biology. 2014; 25-26:43–51. [PubMed: 24445189]
36. Simian M, Hirai Y, Navre M, Werb Z, Lochter a, Bissell MJ. The interplay of matrix metalloproteinases, morphogens and growth factors is necessary for branching of mammary epithelial cells. Development (Cambridge, England). 2001; 128:3117–31.
37. Maller O, Martinson H, Schedin P. Extracellular matrix composition reveals complex and dynamic stromal-epithelial interactions in the mammary gland. 2010:301–18.
38. Weaver VM, Lelièvre S, Lakins JN, Chrenek MA, Jones JCR, Giancotti F, et al. β 4 integrin-dependent formation of polarized three-dimensional architecture confers resistance to apoptosis in normal and malignant mammary epithelium. Cancer Cell. 2002; 2:205–16. [PubMed: 12242153]
39. Wang X, Sun L, Maffini MV, Soto A, Sonnenschein C, Kaplan DL. A complex 3D human tissue culture system based on mammary stromal cells and silk scaffolds for modeling breast morphogenesis and function. Biomaterials. 2010; 31:3920–9. [PubMed: 20185172]
40. Hynes RO. Integrins: Bidirectional, allosteric signaling machines. 2002:673–87.
41. Muschler J, Streuli CH. Cell-matrix interactions in mammary gland development and breast cancer. Cold Spring Harbor perspectives in biology. 2010; 2:a003202–a. [PubMed: 20702598]
42. Raymond K, Faraldo MM, Deugnier MA, Glukhova Ma. Integrins in mammary development. Seminars in Cell and Developmental Biology. 2012; 23:599–605. [PubMed: 22430758]
43. Durbeej M. Laminins. Cell and tissue research. 2010; 339:259–68. [PubMed: 19693542]
44. Marinkovich MP. Tumour microenvironment: laminin 332 in squamous-cell carcinoma. Nature reviews Cancer. 2007; 7:370–80. [PubMed: 17457303]
45. Gjorevski N, Ranga A, Lutolf MP. Bioengineering approaches to guide stem cell-based organogenesis. Development. 2014; 141:1794–804. [PubMed: 24757002]
46. Meinhardt A, Eberle D, Tazaki A, Ranga A, Niesche M, Wilsch-Brauninger M, et al. 3D reconstitution of the patterned neural tube from embryonic stem cells. Stem cell reports. 2014; 3:987–99. [PubMed: 25454634]
47. Sasai Y, Eiraku M, Suga H. In vitro organogenesis in three dimensions: self-organising stem cells. Development. 2012; 139:4111–21. [PubMed: 23093423]
48. Bray LJ, Binner M, Holzheu A, Friedrichs J, Freudenberg U, Hutmacher DW, et al. Multi-parametric hydrogels support 3D in vitro bioengineered microenvironment models of tumour angiogenesis. Biomaterials. 2015; 53:609–20. [PubMed: 25890757]
49. Mercurio AM. Laminin receptors: achieving specificity through cooperation. Trends in cell biology. 1995; 5:419–23. [PubMed: 14732046]

50. Da Silva MS, Horton Ja, Wijelath JM, Blystone LW, Fish WR, Wijelath E, et al. Heparin modulates integrin-mediated cellular adhesion: specificity of interactions with alpha and beta integrin subunits. Cell communication & adhesion. 2003; 10:59–67. [PubMed: 14681057]
51. Faye C, Moreau C, Chautard E, Jetne R, Fukai N, Ruggiero F, et al. Molecular interplay between endostatin, integrins, and heparan sulfate. Journal of Biological Chemistry. 2009; 284:22029–40. [PubMed: 19502598]
52. Gao C, Boylan B, Fang J, Wilcox Da, Newman DK, Newman PJ. Heparin promotes platelet responsiveness by potentiating α IIb β 3-mediated outside-in signaling. Blood. 2011; 117:4946–52. [PubMed: 21368290]
53. Sobel M, Fish WR, Toma N, Luo S, Bird K, Mori K, et al. Heparin modulates integrin function in human platelets. Journal of Vascular Surgery. 2001; 33:587–94. [PubMed: 11241131]
54. Fujisaki H, Hattori S. Keratinocyte apoptosis on type I collagen gel caused by lack of laminin 5/10/11 deposition and Akt signaling. Experimental cell research. 2002; 280:255–69. [PubMed: 12413891]
55. Rousselle P, Keene DR, Ruggiero F, Champliaud MF, Rest M, Burgeson RE. Laminin 5 binds the NC-1 domain of type VII collagen. J Cell Biol. 1997; 138:719–28. [PubMed: 9245798]
56. Shaw KRM, Wrobel CN, Brugge JS. Use of three-dimensional basement membrane cultures to model oncogene-induced changes in mammary epithelial morphogenesis. Journal of mammary gland biology and neoplasia. 2004; 9:297–310. [PubMed: 15838601]
57. Wang X, Reagan MR, Kaplan DL. Synthetic adipose tissue models for studying mammary gland development and breast tissue engineering. Journal of mammary gland biology and neoplasia. 2010; 15:365–76. [PubMed: 20835885]
58. McCaffrey TA, Falcone DJ, Brayton CF, Agarwal LA, Welt FG, Weksler BB. Transforming growth factor-beta activity is potentiated by heparin via dissociation of the transforming growth factor-beta/alpha 2-macroglobulin inactive complex. J Cell Biol. 1989; 109:441–8. [PubMed: 2473082]
59. Mizuno K, Inoue H, Hagiya M, Shimizu S, Nose T, Shimohigashi Y, et al. Hairpin loop and second kringle domain are essential sites for heparin binding and biological activity of hepatocyte growth factor. The Journal of biological chemistry. 1994; 269:1131–6. [PubMed: 8288571]

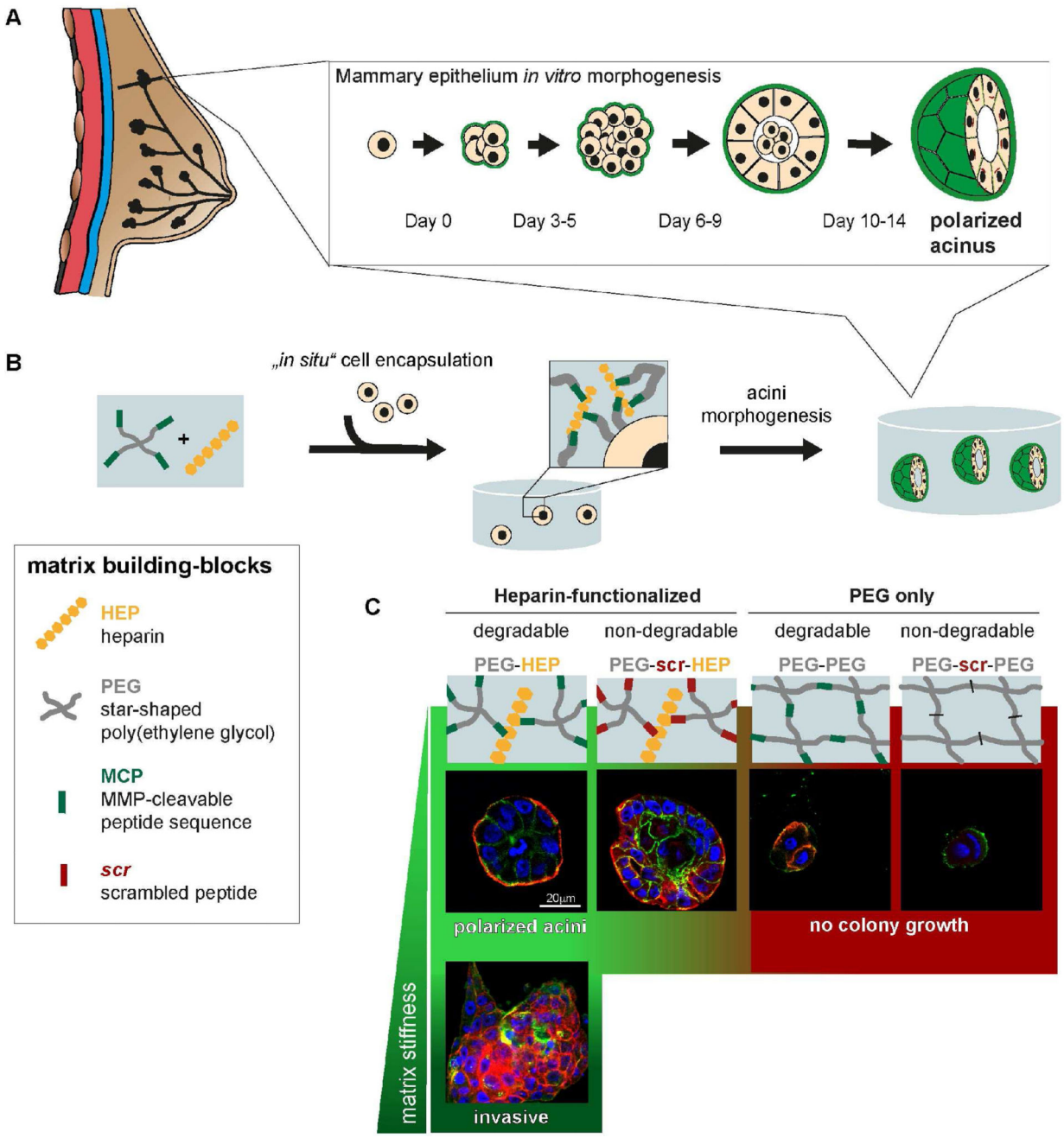

Figure 1. Mammary epithelial cell morphogenesis *ex vivo* in a modular biomimetic hydrogel

(A) Diagram of *in vitro* individual mammary epithelial cell (MEC) morphogenesis into polarized acinus displaying a cleared lumen and basement membrane formation (green). **(B)** Illustration of the study design to investigate MEC morphogenesis in a hydrogel matrix which contains the following building blocks: glycosaminoglycan (GAG) heparin (yellow), MMP-cleavable peptide sequence (MCP, green), non-cleavable scrambled peptide sequence (scr, red) and the inert and star-shaped, four-armed PEG (grey) as a structural matrix component. The versatile and modular chemistry of the biomimetic matrix building blocks facilitates the study of the specific function of the different matrix building blocks and the

exogenous biophysical (mechanical) stimuli on mammary epithelial morphogenesis in a systematic fashion. MECs are embedded as single cells with the modular matrix prior to polymerization. Over 14 days in culture, they undergo morphogenesis to form polarized mammary epithelial acini. (**C**) Polarized MEC acini formation after 14 days in culture is optimal in soft, enzymatically degradable PEG-HEP hydrogels. In each of the other combinations of modular building blocks (e.g. starPEG, heparin, MMP-cleavability) or matrix stiffness, MEC morphogenesis is perturbed. Scale bar = 20 μm.

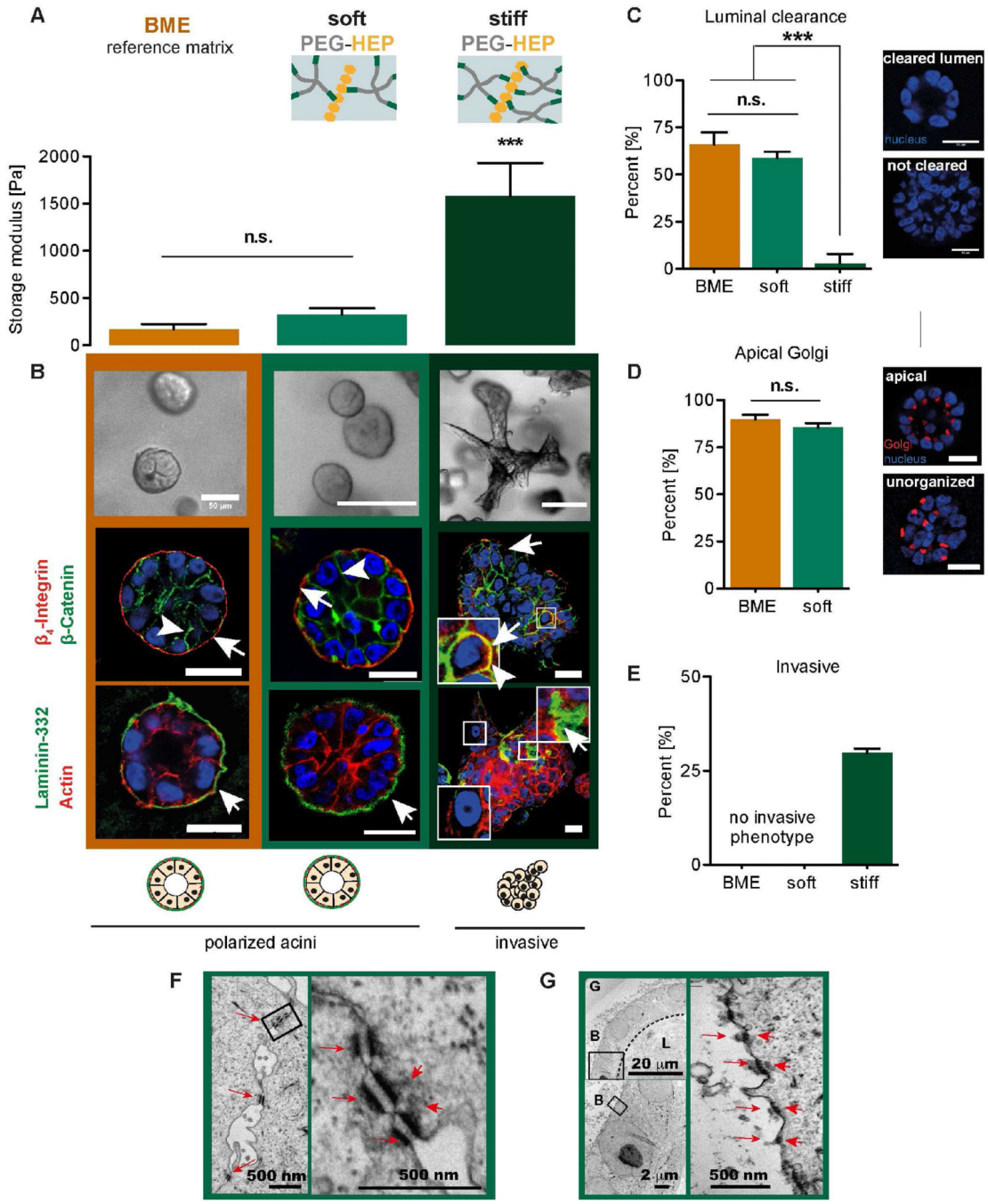

Figure 2. Soft, degradable PEG-HEP matrices support acinar morphogenesis of MECs

(A) Storage modulus (Pa) of BME and soft and stiffPEG-HEP matrices (crosslinking degree of γ=0.63 and γ=1.25, respectively). **(B)** *Top row*: Bright field images of MEC colony morphology after culture in reference BME and soft and stiff PEG-HEP matrices (scale bar = 100 μm). *Middle/bottom row*: Confocal immunofluorescence of polarization markers in MEC colony cross sections from BME and soft and stiff PEG-HEP matrices (scale bar = 20 μm). *Middle row*: Immunofluorescence images of MECs stained for polarity markers β_4-integrin (arrows; red) and β-catenin (arrowhead; green), and nuclei (DAPI; blue). *Bottom*

row: Immunofluorescence images of MECs stained for laminin-332 (arrow; green), actin filaments (red), and nuclei (DAPI; blue). **(C)** *Left:* Percentage of acini containing cleared lumens. *Right*: Representative images of DAPI-stained acini showing luminal clearance. **(D)** *Left:* Percentage of acini containing apically oriented Golgi apparatus. *Right*: Representative images of GM-130- (Golgi apparatus) and DAPI-stained (nucleus) acini showing orientation of the Golgi relative to the nuclei. **(E)** Percentage of acini showing an invasive (non-spherical) phenotype. **(F and G)** Ultra-structural analysis of MECs cultured in soft PEG-HEP matrices. **(F)** Left image shows several desmosomes (red arrows) at the epithelial cell-cell interface (scale bar = 500 nm). Right image is a magnified inset of the left image showing the desmosomes (red arrows) with connected cytoplasmic filaments (red arrowheads, scale bar = 500 nm). **(G)** The top left overview image is a representative MEC colony with cleared lumen (L). Note that the hydrogel (G) polymeric network appears degraded in the periphery of the basal (B) acini surface (scale bar = 20 μm). The left bottom image is a magnified inset of the left top image (scale bar = 2 μm). The right image is further magnified at the cell-matrix interface, showing the typical dense dark structures of hemidesmosomes (arrows), which are connected to cytoplasmic filaments (arrowheads, scale bar = 500 nm). G = gel, L = lumen, B = basal side of acini. A, C, D and E are mean ± S.D. (A) ANOVA with Tukey's multiple comparison, n = 3. (C) and (D) n = 50 acini counted from three independent experiments; un-paired t-test. (E) n = 100-150 from one representative experiment; Kruskal-Wallis test with Dunn's multiple comparisons. All images and measurements in this figure are of cells after 14 days in culture. n.s. = not significant; $p \geq 0.05$; ** $p < 0.01$; *** $p < 0.001$.

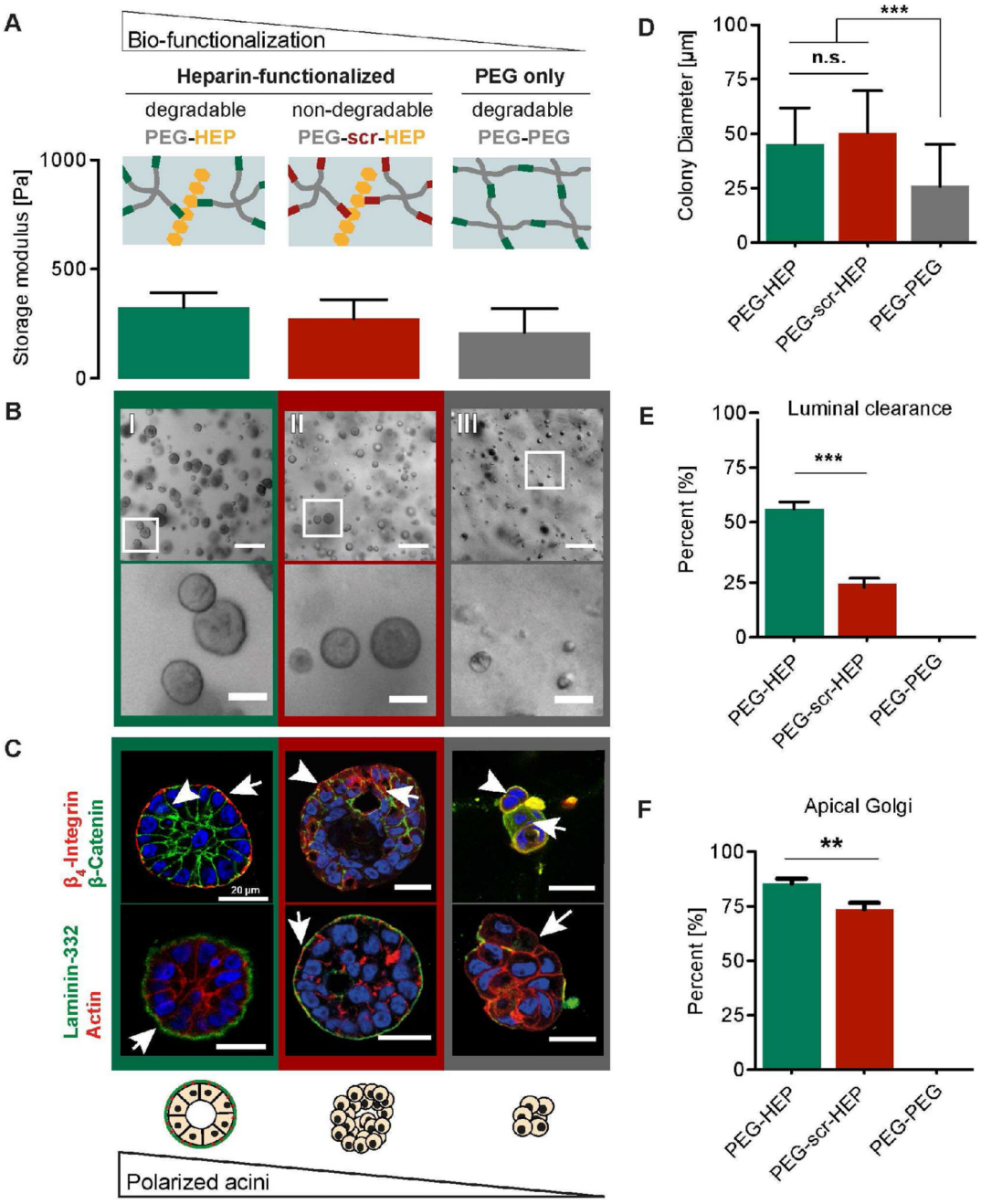

Figure 3. Impact of matrix degradability and GAG integration on MEC morphogenesis

(A) Storage modulus (Pa) of matrices with decreasing biomolecular polymer network functionalization. *Left to right*: MMP-cleavable PEG-HEP, MMP-insensitive PEG-scr-HEP, and MMP-cleavable PEG-PEG matrices. **(B)** Bright field images showing the colony morphology of MECs grown in soft synthetic matrices with different degrees of biofunctionality: (I) PEG-HEP, (II) PEG-scr-HEP, and (III) PEG-PEG matrices (scale bar = 200 μm). *Bottom row:* magnified image of the white box in top row (scale bar = 50 μm). **(C)** Confocal immunofluorescence images of MEC colony cross sections grown in the different matrices (as in B, scale bar = 20 μm). *Top row*: Immunfluorescence of β_4-integrin (arrows;

red), β-catenin (arrowhead; green), and nuclei (DAPI; blue). *Bottom row*: Immunfluorescence of the basement membrane protein laminin-332 (arrows; green), actin filaments (red), and nuclei (blue) **(D)** MECs were grown in PEG-MCP-HEP, PEG-scr-HEP, or PEG-MCP-PEG matrices, brightfield images were taken, and the colony diameters measured. **(E)** Percentage of acini containing cleared lumens. **(F)** Percentage of acini containing apically oriented Golgi apparatus. A, D, E and F are mean ± S.D. (A) ANOVA with Tukey's multiple comparison, n = 3; (E) and (F) unpaired t-test, n = 50 from three independent experiments. (D) Kruskal-Wallis test with Dunn's multiple comparisons; n= 100-150 from one representative experiment. All images and measurements in this figure are of cells after 14 days in culture. n.s. = not significant ($p \geq 0.05$), ** $p < 0.01$, *** $p < 0.001$.

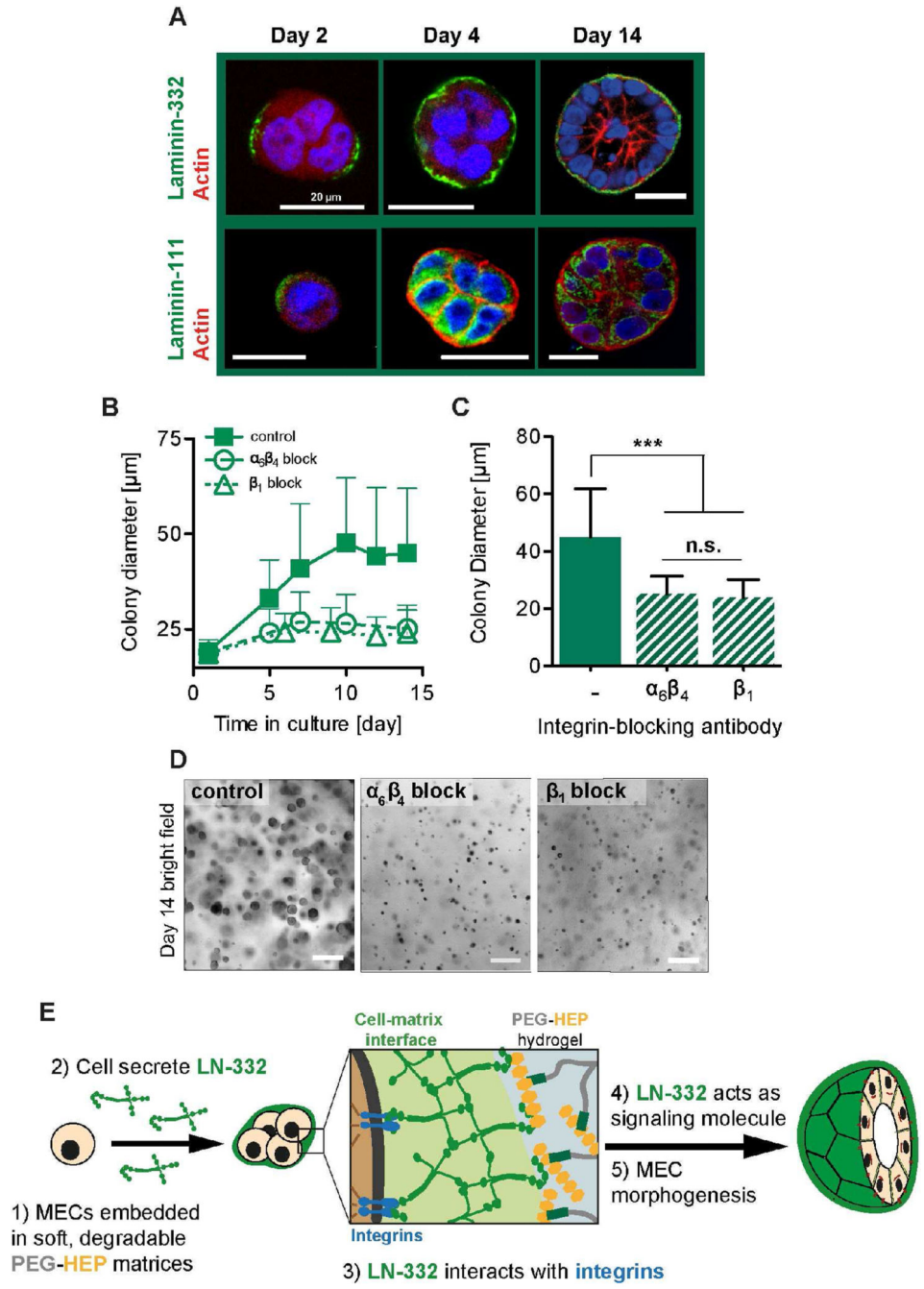

Figure 4. Mechanism of MEC morphogenesis in soft, degradable PEG-HEP matrices through basement membrane assembly and functional integrin block

(A) Top row: Confocal immunofluorescence images of laminin-332 (top, green) or laminin-111 (bottom, green) expression in MEC colonies grown in soft, degradable PEG-HEP hydrogels for the number of days indicated (scale bar = 20 μm). *Top row*: After two days laminin-332 was deposited partially around the outer colony surface. By day 4 of culture, laminin-332 appears fully distributed around the outer acini surface (actin filaments, red; nuclei, blue). *Bottom row*: No extracellular laminin-111 deposition was observed in the cultures. **(B)** MECs were grown in soft, degradable PEG-HEP matrices in the presence or

absence of β_1 or $\alpha_6\beta_4$ integrin blocking antibodies. Brightfield images were taken, and the colony diameters measured. MEC colony growth, as measured by brightfield microscopy, is impaired by blocking β_1 or $\alpha_6\beta_4$ integrin function. **(C)** Colony diameter after 14 days. Kruskal-Wallis test with Dunn's multiple comparisons, n = 130-150 from one representative experiment. n.s. = not significant ($P \geq 0.05$); *** $P < 0.001$. **(D)** Bright field images of MECs grown in soft, degradable PEG-HEP matrices after treatment with integrin blocking antibodies (β_1 or $\alpha_6\beta_4$; scale bar = 20 μm). **(E)** Diagram of the hypothesized mechanism of polarized acini development in soft, degradable PEG-HEP matrices. MECs embedded within soft, enzymatically degradable PEG-HEP hydrogels constitutively secrete LN-332, which binds to heparin and through binding to integrins acts as a signaling molecule to promote MEC morphogenesis into polarized acini.

Table 1

Definitions and acronyms of all biohybrid materials used in this work

PEG-HEP hydrogels are MMP-cleavable heparin-based hydrogels comprised of PEG-MCP and HEP-Mal precursors. PEG-scr-HEP are MMP-insensitive heparin-based hydrogels comprised of the precursors PEG-scr and HEP-Mal. PEG-PEG defines MMP-cleavable PEG-based hydrogels comprised of the precursors PEG-MCP and PEG-Mal. PEG-scr-PEG represents MMP-insensitive PEG-based hydrogels comprised of the precursors PEG-scr and PEG-Mal. PEG-MCP is four-armed star-shaped polyethylene glycol (PEG) maleimide (PEG-Mal, MW: 10080, JenKem) functionalized with the MMP-cleavable (MCP) peptide sequence (GCG GPQG↓IWGQ GGCG). HEP-Mal is heparin that is functionalized with 6 maleimide groups per molecule. PEG-scr is starPEG functionalized with the MMP-insensitive scrambled *(*scr*)* peptide sequence (GCG IGQGQGPW GGCG). PEG-Mal is four-armed starPEG that contains a maleimide terminal group on each PEG arm.

Acronym	Enzymatically Degradable?	Polymer Building Blocks
PEG-HEP	Yes	PEG-MCP + HEP-Mal
PEG-scr-HEP	No	PEG-scr + HEP-Mal
PEG-PEG	Yes	PEG-MCP + PEG-Mal
PEG-scr-HEP	No	PEG-scr + PEG-Mal